Neutron Scattering by Magnons of an Antiferromagnet with Modulated Spin Amplitudes

T. Wolfram and S. Ellialtioglu[a]
Department of Physics, University of Missouri–Columbia, Columbia, Missouri 65211
(Received 7 January 1980)

Neutron scattering by the magnons of a spin-density-wave antiferromagnet is investigated with a one-dimensional local-moment model with long-range exchange. The magnon dispersion curves are unusual and the neutron inelastic scattering cross section exhibits peaks at a variety of nuetron momentum transfers including the commensurable and incommensurable points. The general features of the calculation correlate remarkably well with recent neutron inelastic scattering data on chromium and strongly suggest a new interpretation of the data.

PACS numbers: 75.25.+z, 75.50.Ee, 61.12.Fy

In a recent Letter Fincher, Shirane, and Werner[1] reported neutron inelastic scattering results for antiferromagnetic chromium with an incommensurable spin-density wave[2] of wave vector $\vec{Q}$ along the [001] direction. They observed a low-energy (4-meV) peak for neutron momentum transfer $\vec{K} = \vec{X} \equiv (2\pi/a)(0, 0, 1)$ as well as the expected peaks centered around $(2\pi/a)(0, 0, 1 \pm \epsilon)$, where ϵ describes the modulation of the spin-density wave in chromium [$\vec{Q} = (2\pi/a)(0, 0, 1 - \epsilon)$ and $\vec{a}$ is the bcc lattice parameter]. The appearance of a low-energy peak at $\vec{X}$ was surprising since the magnon dispersion curves of chromium[2-4] were thought to rise linearly from the points $(2\pi/a)(0, 0, 1 \pm \epsilon)$ with a very large velocity[5] ($\hbar C = 1000$ meV Å) and therefore they should provide no low-energy magnons at $\vec{X}$. Fincher, Shirane, and Werner[1] also observed an anomalous rise in the background counting rate with increasing temperature for the scattering at X. Based on these observations they speculated that the 4-meV peak was associated with large-amplitude fluctuations of blocks of spins.

In this Letter we present the results of a study of a simple modulated local spin model which shows that the magnon dispersion curves are unusual and produce very complex structures in the neutron inelastic scattering cross section. The model results for the neutron scattering law exhibit many of the features observed for chromium and suggest that the 4-meV peak is due to magnons near the commensurable point.

The modulated spin configuration of chromium is shown schematically in the inset of Fig. 1. The planes of spins, in the y direction, have amplitudes that are modulated along the z direction. For magnon propagation along $\vec{Q}$ we can approximate the system by a linear array of spins whose amplitudes are given by $s^x(n) = s^0 \times \cos\frac{1}{2}Q(n+d)a$, where s^0 is a spin amplitude, n is an integer, d is an arbitrary phase shift, $\frac{1}{2}a$ is the nearest-neighbor distance and Q is the magnitude of Q. For Q near to $2\pi/a$, $s^x(n)$ describes a sinusoidally modulated array with the spins antiferromagnetically aligned except across the nodes where pairs of spins are parallel as in

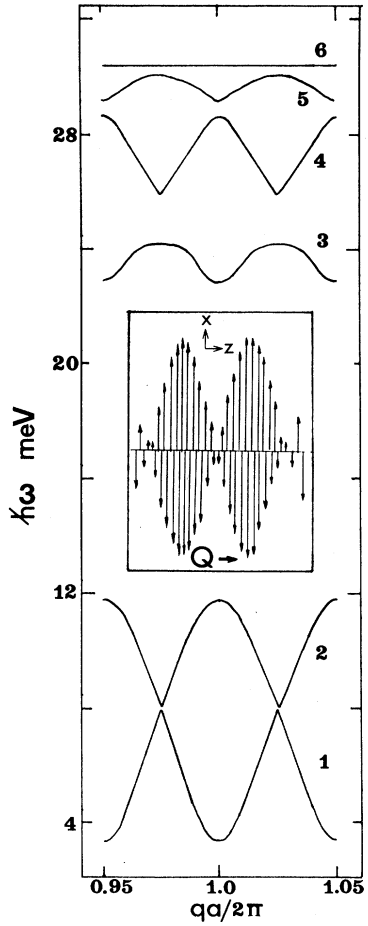

FIG. 1. Magnon dispersion curves. The inset shows the modulated spin configuration for chromium.

Fig. 1. For chromium, Q is $0.9515(2\pi/a)$ at low temperatures[1] (and is slightly temperature dependent) so that there are about 40 spins in each modulation period. For $Q=0.95(2\pi/a)$ the spin array would be periodic with exactly 40 spins in each unit cell. This suggests approximating the actual system by a periodic array with 40 spins in each unit cell.

We use the Hamiltonian

$$H=\tfrac{1}{2}\sum_{n\neq n'}\sum J(n,n')\vec{s}(n)\cdot\vec{s}(n') - \sum_{n} H_a b_n s^x(n), \quad (1)$$

where $J(n,n')$ is the exchange interaction, H_a is a uniaxial anisotropy energy and $b_n=\mathrm{sgn}[\cos\tfrac{1}{2}q(n+d)a]$. The exchange interaction is assumed to be long range and of the form

$$J(n,n')=-b_n b_{n'} J^0 \exp\{-\lambda|n-n'|-1|\}, \quad J^0>0. \quad (2)$$

In order that the assumed spin-density wave be stable to magnon excitations the long-range exchange interaction must reflect the orientation of the spins of the spin-density wave. The prefactor $-b_n b_{n'}$ ensures that the pair interaction energy is negative for the assumed ground-state distribution. The parameters J^0 and λ fix the energy scale and the range of the exchange interaction.

Because of the assumed periodicity we can write $s(n)=s(p,j)$, where p is the unit-cell number and $j=1,2,\ldots,40$ labels the spins within a cell. We introduce the operators $A(q,j)$ defined by

$$A(q,j)=N^{-1/2}\sum_{p=1}^{N}[2s^0C_j(Q)]^{-1/2} \times\exp(iqpD)[s^z(p,j)+is^y(p,j)], \quad (3)$$

where N is the number of unit cells, $C_j(Q)=|\cos\tfrac{1}{2}Q(j+d)a|$, $D=40(a/2)$ is the length of the unit cell and q is the magnon wave number. The usual equations-of-motion method[6] yields a 40×40 matrix equation of the form

$$\sum_{j'}\{M_{j,j'}(q)-\hbar\omega_{j,j'}(q)\}A^+(q,j')=0, \quad (4)$$

where $M_{j,j'}(q)$ specifies the interaction matrix elements. The eigenvalues $\hbar\omega_t(q)$ with $t=1,2,\ldots,20$ occur in pairs: $\hbar\omega_t(q)=-\hbar\omega_{-t}(q)$. The eigenoperators, $L^+(q,t)$, are related to the $A^+(q,j)$ operators by

$$L^+(q,t)=\sum_j V_{j,t}(q)A^+(q,j), \quad (5)$$

where $V_{j,t}(q)$ are the components of the eigenvectors of the matrix M. They satisfy the normalization condition

$$\sum_j V_{j,t}(q)\,b_j\,V_{j,t'}{}^*(q)=\mathrm{sgn}\omega_t(q), \quad (6)$$

and diagonalize the Hamiltonian (neglecting fourth-order terms). The quantities, $[2s^0C_j(Q)]^{1/2}V_{j,t}(q)$, specify the relative amplitudes of spin motion for a magnon with wave number q and branch number t.

Figure 1 shows a graph of the first six positive-frequency branches of a typical magnon dispersion curve. For the example shown, $H_a=0.16$ meV, $J^0s^0=16$ meV, $d=0.14$, and $\lambda=0.5$. The dispersion curves are repeated in each large unit-cell zone. In general, the dispersion decreases rapidly with increasing branch number. For the case shown in Fig. 1 there is little dispersion for $t=6$. Branches $t=7$–20 (not shown) are flat and the maximum energy for $t=20$ is 82.6 meV.

The behavior of the lowest branch is similar to that expected for a spin-density-wave antiferromagnet[3,4] for q near to the incommensurable points ($qa/2\pi\approx0.95$ or 1.05), but the behavior away from these points and the existence of multiple branches and energy gaps cannot be obtained from the usual model for an itinerant antiferromagnet.

For $H_a\ll J^0s^0$, the qualitative features of the dispersion curves do not depend strongly on any of the parameters except Q. The particular values of the parameters used for Fig. 1 were selected so that the neutron inelastic scattering corresponds to that observed for chromium, as described below.

For the model considered here the scattering function, $S(K,\omega)$, for one-magnon inelastic neutron scattering can be reduced to the form

$$S(K,\omega)=B\sum_{t>0}T_t(K)\{n_t(K)\delta(\omega+\omega_t(K))+[n_t(K)+1]\delta(\omega-\omega_t(K))\}, \quad (7)$$

where B is a constant, K is the magnitude of the neutron momentum transfer along $\vec{Q}$, $n_t(K)$ is the magnon occupation probability and

$$T_t(K)=\sum_j\sum_{j'}\{V_{j,t}(K)V_{j',t}{}^*(K)V_{j,-t}(K)V_{j',-t}{}^*(K)\}[C_j(Q)C_{j'}(Q)]^{1/2}\exp[\tfrac{1}{2}iK(j-j')a]. \quad (8)$$

The function $T_t(K)$ is symmetric about $Ka = 2\pi$ and for the lower branches ($t \leq 6$) is significant only in the range $0.9 \lesssim Ka/2 \lesssim 1.1$. For $\hbar\omega \lesssim 30$ meV the average value of $T_t(K)$ decreases with increasing t. For $t = 1$, $T_1(K)$ is peaked at $Ka/2\pi = 0.95$, decreases to zero at 1.0, and has structure at intermediate values of K. On the other hand, $T_2(K)$ is large at both 1.0 and 0.95 but peaked at an intermediate value of K. In general, the peaks in $T_t(K)$ are due to constructive interference between the neutron wave and the complex (nonsinusoidal) spin "motions" described by the magnon eigenvectors. It is clear that $S(\boldsymbol{K}, \omega)$ will have a complicated behavior with peaks at a variety of K values including both Q and $2\pi/a$.

In order to compare the predicted scattering with the experimental data for chromium we introduce the function $\langle S(K, \omega)\rangle$, which is the convolution of $S(K, \omega)$ with a Gaussian resolution function having full-width-at-half-maximum parameters, $\Delta K = 0.005(2\pi/a)$ and $\Delta\hbar\omega = 1.2$ meV. The values of ΔK and $\Delta\hbar\omega$ are consistent with those of the Cr data.

The results for $\langle S(K, \omega)\rangle$ for a temperature of 200 K are shown in Fig. 2. The patterns are symmetric about $K = 2\pi/a$ and the intensity is significant only for $Ka/2\pi$ between 0.900 and 1.100 even though the dispersion curves repeat in each zone.

It is important to note that the peak in $\langle S(K, \omega)\rangle$ for 4 meV around $Ka/2\pi = 1.0$ is a result of scattering from K's near $2\pi/a$ which are included in the resolution function [$S(K, \omega)$ itself is zero at $K \equiv 2\pi/a$]. The peaks in $\langle S(K, \omega)\rangle$ for 8 meV, however, are directly related to peaks in $S(K, \omega)$.

In Fig. 3(a), a comparison with the data of Fincher, Shirane, and Werner[1] is given with $\langle S(K, \omega)\rangle$ normalized to the same scale as the data. The agreement is seen to be very good, especially considering the simplicity of the model. The peaks in $\langle S(K, \omega)\rangle$ are at $Ka/2\pi = 0.9525$, 1.0000, and 1.0475. The outer peaks in the data are shifted from those of theory. This difference is, in part, due to the fact that the experimental Q is larger than the value of $0.95(2\pi/a)$ assumed in the calculation. The peak in the data around 1.0 is less well resolved than in the theoretical curve. This may be due to the scattering from $\vec{K}$'s off the $\vec{Q}$ axis which lie within the experimental resolution ellipsoid. The asymmetry in the data about 1.0 is due to the effect of the form factor, an effect not included in the theo-

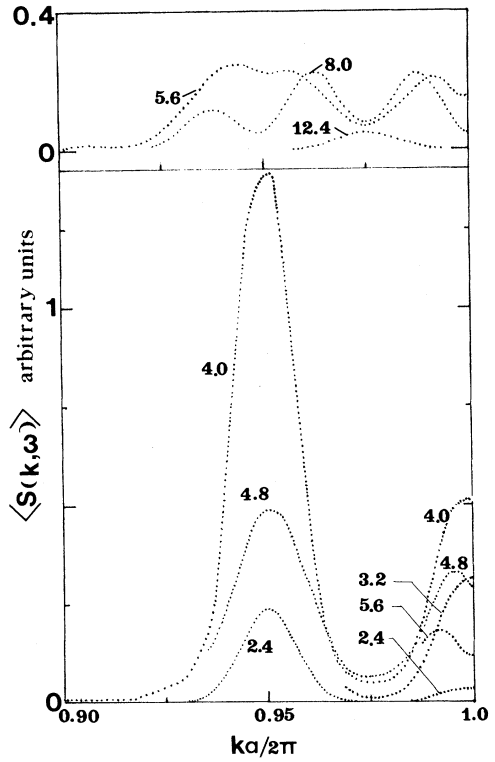

FIG. 2. Constant-energy scans for several energies for $\langle S(K, \omega)\rangle$ as a function of the neutron momentum transfer.

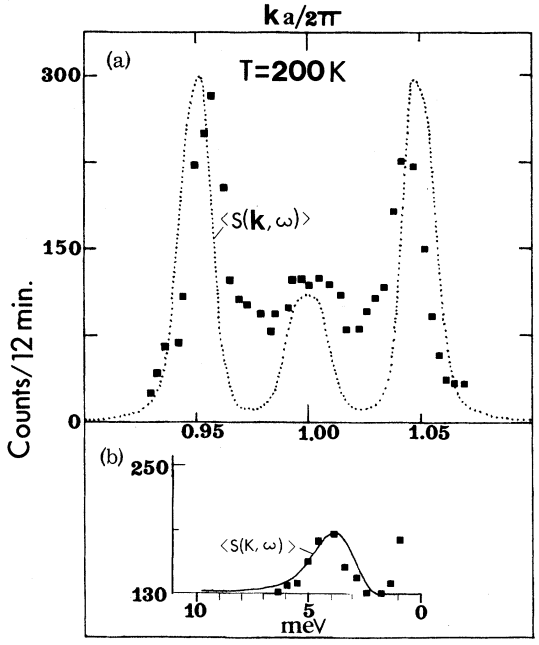

FIG. 3. (a) Comparison of $\langle S(\boldsymbol{K}, \omega)\rangle$ with the neutron data (Ref. 1) for Cr at 4 meV and 200 K. (b) Comparisons with the data for $\boldsymbol{K} = (2\pi/a)(0, 0, 1)$ at a temperature of 200 K.

retical curves.

A comparison of the theoretical results (normalized at 4 meV) with the experimental constant-K scan at $(2\pi/a)(0, 0, 1)$ is shown in Fig. 3(b). A constant background of (130 counts)/(12 min) has been added to the theoretical results. The correlation is quite good. The rise in scattering intensity at very low energy is not given by the theory but the peak at 4 meV and the subsequent falloff is well represented.

The results presented here strongly suggest low-energy magnon modes exist near to $K = 2\pi/a$ and that the scattering peak observed at $2\pi/a$ for chromium is due to the presence of (small-amplitude) magnon modes rather than large-amplitude fluctuations of blocks of spins as suggested by Fincher, Shirane, and Werner[1]. This conclusion does not rule out the possibility that large-amplitude excitations also exist in chromium. The results presented here do not account for the large increase in the background scattering with temperature which Fincher, Shirane, and Werner[1] observed.

The model discussed here is clearly too simple to provide a precise description of chromium and the details of our calculation should not be regarded as accurate. A model including the three-dimensional magnon dispersion, the large anisotropy[7] which confines the spin motions to the plane perpendicular to $\vec{Q}$ as well as the experimental three-dimensional resolution function will be required in order to provide a satisfactory analysis of the chromium data. Nevertheless, our results establish a number of important physical properties of a modulated spin system which must be present in any model: (1) The magnon spectrum is complex, contains a number of energy gaps, and has low-energy modes near the commensurable point. (2) Peaks in $S(K, \omega)$ arise from interference between the neutron wave and the nonsinusoidal magnon spin "motions" and can occur at a variety of $\vec{K}$ vectors, including the commensurable point. (3) Peaks in $\langle S(K, \omega)\rangle$ may be produced by unresolved structures in $S(K, \omega)$ and do not necessarily imply a special feature in the magnon dispersion curve.

The considerations discussed here will also be of importance in understanding neutron scattering from other spin modulated systems including erbium and thulium.[8]

The authors wish to thank Professor S. A. Werner for suggesting this problem and for useful discussions. This research was supported in part by a grant from the National Science Foundation.

---

[a]On leave from the Middle East Technical University, Ankara, Turkey.

[1]C. R. Fincher, Jr., G. Shirane, and S. A. Werner, Phys. Rev. Lett. 43, 1441 (1979).

[2]A. W. Overhauser, Phys. Rev. 128, 1437 (1962).

[3]P. A. Fedders and P. C. Martin, Phys. Rev. 143, 245 (1966).

[4]S. H. Liu, Phys. Rev. B 2, 2664 (1976).

[5]S. K. Sinha, S. H. Liu, L. D. Muhlestein, and N. Wakabayashi, Phys. Rev. Lett. 23, 311 (1969).

[6]W. Marshall and S. W. Lovesey, *Theory of Thermal Neutron Scattering* (Oxford Univ. Press, Oxford, England, 1971).

[7]S. A. Werner, A. S. Arrot, and H. Kendrick, Phys. Rev. 155, 528 (1967).

[8]For a review of the spin structures in rare-earth metals, see S. K. Sinha, in *Handbook on the Physics and Chemistry of Rare Earths*, edited by K. A. Gschneider, Jr., and L. Eyring (North Holland, Amsterdam, 1978), Chap. 7.

ERRATUM

BAND-TAIL ABSORPTION IN HYDROGENATED AMORPHOUS SILICON. Richard S. Crandall [Phys. Rev. Lett. 44, 749 (1980)].

Reference 1 should read

[1]P. G. LeComber, A. Madan, and W. E. Spear, in *Electronic and Structural Properties of Amorphous Semiconductors*, edited by P. G. LeComber and J. Mort (Academic, New York, 1973), p. 373; T. Suzuki, M. Hirose, S. Ogose, and Y. Osaka, Phys. Status Solidi (a) 42, 337 (1977); R. S. Crandall, J. Non-Cryst. Solids 35/36, 281 (1980); J. I. Pankove, F. H. Pollak, and C. Schnabolk, J. Non-Cryst Solids 35/36, 459 (1980); D. A. Anderson, G. Moddel, and W. Paul, J. Non-Cryst. Solids 35/36, 345 (1980); G. D. Cody, B. Abeles, C. R. Wronski, B. Brooks, and W. A. Lanford, J. Non-Cryst. Solids 35/36, 463 (1980).